Metabolic Engineering 14 (2012) 242–251

Contents lists available at SciVerse ScienceDirect

Metabolic Engineering

journal homepage: www.elsevier.com/locate/ymben

Spatial organization of enzymes for metabolic engineering

Hanson Lee [a,b], William C. DeLoache [a], John E. Dueber [a,b,*]

[a] Department of Bioengineering, University of California, Berkeley, Berkeley, CA 94720, USA
[b] Energy Biosciences Institute, University of California, Berkeley, Berkeley, CA 94720, USA

ARTICLE INFO

Available online 18 September 2011

Keywords:
Synthetic scaffolds
Metabolite microdomains
Compartmentalization
Protein shells
Shell pores

ABSTRACT

As synthetic pathways built from exogenous enzymes become more complicated, the probability of encountering undesired interactions with host organisms increases, thereby lowering product titer. An emerging strategy to combat this problem is to spatially organize pathway enzymes into multi-protein complexes, where high local concentrations of enzymes and metabolites may enhance flux and limit problematic interactions with the cellular milieu. Co-localizing enzymes using synthetic scaffolds has improved titers for multiple pathways. While lacking physical diffusion barriers, scaffolded systems could concentrate intermediates locally through a mechanism analogous to naturally occurring microdomains. A more direct strategy for compartmentalizing pathway components would be to encapsulate them within protein shells. Several classes of shells have been loaded with exogenous proteins and expressed successfully in industrial hosts. A critical challenge for achieving ideal pathway compartmentalization with protein shells will likely be evolving pores to selectively limit intermediate diffusion. Eventually, these tools should enhance our ability to rationally design metabolic pathways.

1. Introduction

Metabolic engineering holds promise as an alternative to synthetic chemistry for cheaply and renewably producing molecules of value. Although construction of novel pathways out of enzymes from different organisms proves to be a powerful strategy for synthesizing a variety of compounds (reviewed in Keasling, 2010), achieving commercially viable productivity remains challenging. Some of these challenges are attributable to low enzymatic activities and flux imbalances, while others often arise from unintended and difficult-to-characterize interactions between synthetic pathways and the cellular environment of host organisms. For example, pathway metabolites may be toxic to the host organism, get diverted by endogenous reactions, or be lost via secretion (Fig. 1A). An emerging strategy to combat these issues is to organize enzymes of a synthetic pathway into multi-enzyme complexes. Co-localizing pathway enzymes into complexes with optimal enzyme stoichiometries increases the local concentrations of pathway metabolites and enzymes, potentially limiting the accumulation of pathway intermediates and decreasing the probability of unintended interactions with other cellular components (Fig. 1B).

Multi-enzyme complexes are frequently seen in nature. Enzymes catalyzing the last two steps of tryptophan synthesis form a complex where the intermediate indole is channeled from one active site to the other (Miles, 2001). Larger enzyme complexes are prevalent in eukaryotes (An et al., 2008; Narayanaswamy et al., 2009; Noree et al., 2010). An especially interesting case is the purinosome, which assembles dynamically depending on the cellular purine level (An et al., 2008). Bacteria encapsulate vital pathways such as carbon fixation in polyhedral nanostructures called microcompartments (Shively and English, 1991; Yeates et al., 2010), and eukaryotes have multiple membrane-bound organelles, which insulate various biochemical processes. While enzyme co-localization occurs in all of these examples, naturally occurring enzyme complexes appear to employ a variety of mechanisms by which they confer a selective advantage. For instance, bacterial microcompartments in *Salmonella enterica* trap a toxic aldehyde intermediate and limit its buildup in the cell (Sampson and Bobik, 2008). Evolutionarily related microcompartments in cyanobacteria concentrate CO_2 around carbon fixation enzymes to increase reaction rates (Dou et al., 2008; Marcus et al., 1992). Mechanisms of other natural enzyme complexes were reviewed recently (Conrado et al., 2008). Better understanding of the mechanisms behind enzyme complexes will help inform and inspire more effective engineering of multi-enzyme complexes.

As a first attempt to organize enzymes into complexes, fusions of metabolic enzymes catalyzing successive reactions were shown to enhance pathway flux in certain instances (reviewed in Conrado et al., 2008). However, two notable disadvantages are inherent to the enzyme fusion strategy: it is not readily amenable

* Corresponding author at: Department of Bioengineering, University of California, Berkeley, Berkeley, CA 94720, USA. Fax: +1 510 642 9725.
E-mail address: jdueber@berkeley.edu (J.E. Dueber).

1096-7176/$ - see front matter © 2011 Elsevier Inc. All rights reserved.
doi:10.1016/j.ymben.2011.09.003

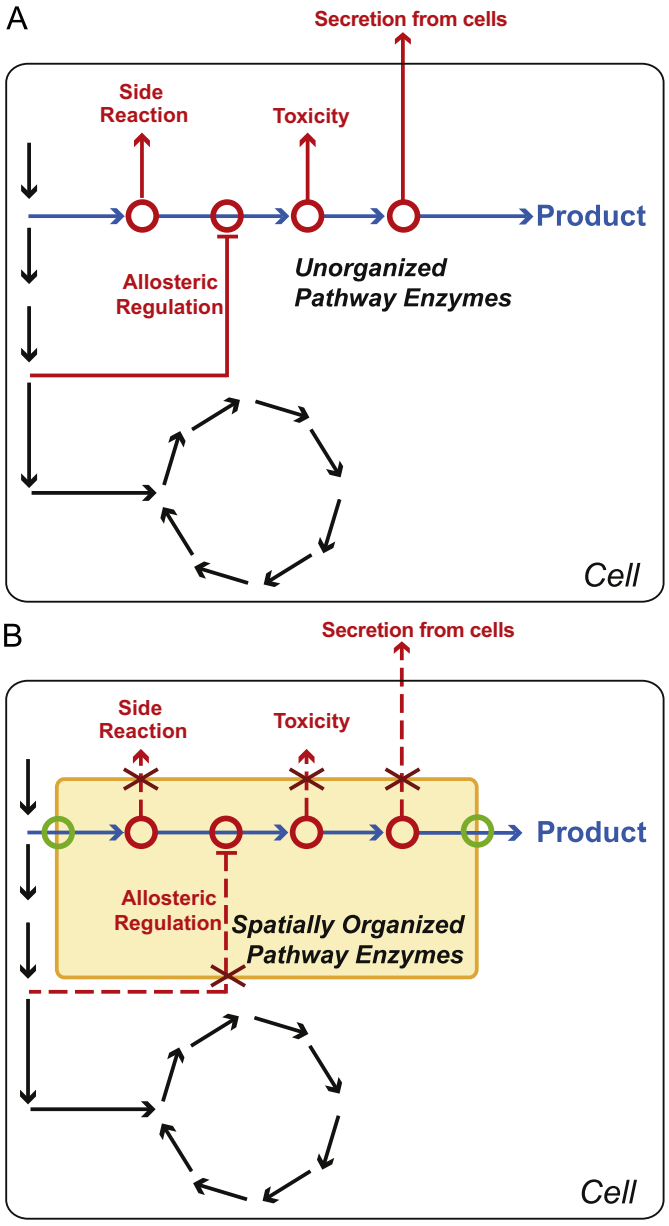

Fig. 1. Many problems associated with engineered metabolic pathways could be mitigated by generating multi-enzyme complexes. Synthetic pathways are often constructed by introducing heterologous enzymes (blue arrows) to an industrial host organism. Host metabolism (black arrows) can have undesirable interactions with these engineered pathways, including metabolite toxicity, intermediate loss via secretion or side reactions, and unwanted allosteric regulation (red lines, Fig. 1A). These problems potentially can be alleviated by organizing pathway enzymes into multi-protein complexes (orange rectangle, Fig. 1B), where the local metabolism within the complex is decoupled from the global metabolism of the cell except at specific points such as substrate entry and product exit (green circles). This strategy could be scaled up to allow for multiple non-interacting complexes in a single cell. (For interpretation of the references to colour in this figure legend, the reader is referred to the web version of this article.)

to pathways containing more than two enzymes, and it cannot be easily used to balance enzyme stoichiometry. We therefore focus our review on two emerging alternatives. The first is synthetic scaffolding, a flexible method to co-localize two or more pathway enzymes and balance their stoichiometry at the complex. Although still under active characterization, we propose here one possible mechanism through which scaffolded enzymes could reduce intermediate buildup within the cell. In the second section, we discuss the potential for the use of protein shells to enable more advanced spatial organization of metabolic enzymes. Shell proteins create a physical barrier to prevent intermediates from escaping, while pores allow substrate(s) to enter and product(s) to exit. We conclude with a discussion of the advantages and associated challenges inherent to both of these technologies.

2. Modular scaffold strategy for improving metabolic flux

Recently the utilization of synthetic scaffold proteins to organize enzymes into complexes was shown to considerably increase titers of the mevalonate and glucaric acid biosynthetic pathways (Dueber et al., 2009; Moon et al., 2010). In both cases, a scaffold protein carrying multiple protein–protein interaction domains was used to co-localize sequential pathway enzymes that had been tagged with peptide ligands specific for the domains on the scaffold (Fig. 2A). By varying the number of domains on the synthetic scaffold, the relative ratio of recruited enzymes was controlled. A major drawback to enzyme–enzyme fusions is that they often result in decreased enzymatic activity for one or both enzymes. This modular scaffolding strategy results in less severe perturbation to enzymes of interest since it only requires the addition of a short peptide to each pathway enzyme. It also provides control over stoichiometry to balance reaction fluxes, a parameter we found to be a critical determinant of scaffold effectiveness.

2.1. Use of modular protein interaction domains to spatially organize enzymes

Many signaling proteins, adapters, and scaffolds contain modular protein–protein interaction domains. When isolated, these domains independently fold with N- and C-terminus that are surface-exposed, close together, and removed from the binding pocket allowing them to maintain binding function when recombined as an internal fusion or to the N- or C-terminus of another protein (Pawson and Nash, 2000). They specifically bind other domains or short peptides on target proteins with intermediate affinity (K_d in the 0.1–10 μM range) (Posern et al., 1998; Tonikian et al., 2008). It was previously shown that these modular domains can be recombined in order to predictably engineer new combinations of protein–protein interactions (Dueber et al., 2004; Peisajovich et al., 2010; Remenyi et al., 2006). Similar control can be gained for DNA–protein interactions by the use of zinc finger domains that have been engineered to bind specific DNA sequences (Maeder et al., 2008). Both protein–protein and DNA–protein interactions have been used to co-localize metabolic enzymes to improve pathway flux as discussed below.

2.2. Demonstration of feasibility

As a first testbed for utilizing modular protein–protein interaction domains to form mutli-enzyme complexes, the mevalonate biosynthetic pathway consisting of acetoacetyl-CoA transferase (atoB), hydroxy-methylglutaryl-CoA synthase (HMGS), and hydroxy-methylglutaryl-CoA reductase (HMGR) was used by our laboratory in collaboration with Dr. Jay Keasling. This pathway, which produces mevalonate from acetyl-CoA, suffers from a flux imbalance between HMGS and HMGR that results in the accumulation of the intermediate HMG-CoA (Pitera et al., 2007). HMG-CoA has been demonstrated to be highly cytotoxic to the production host, *Escherichia coli* (Kizer et al., 2008; Pitera et al., 2007). We began with an engineered direct co-recruitment between HMG-CoA producing and consuming enzymes (HMGS and HMGR, respectively). A varying number of SH3 ligands were fused to the C-terminus of HMGS and an N-terminal SH3 domain was tethered to HMGR. A 10-fold improvement in

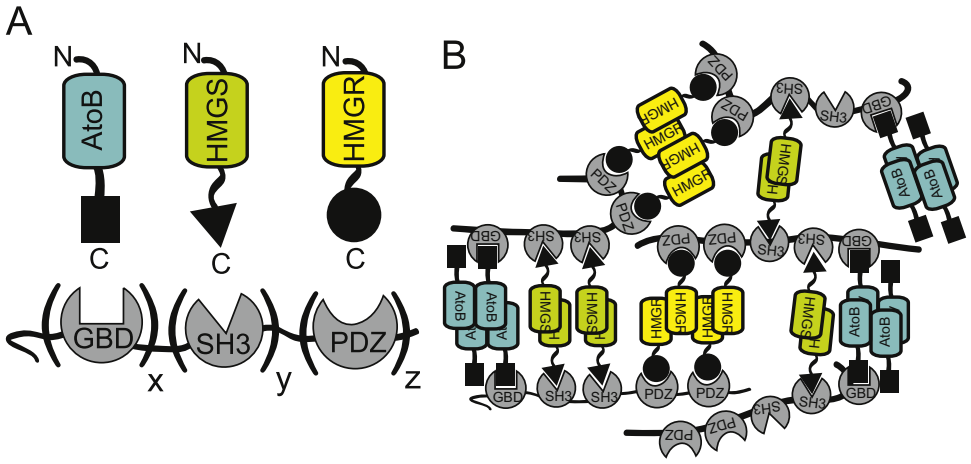

Fig. 2. Schematic of a synthetic scaffolding strategy. (A) A synthetic scaffold was constructed with three modular protein–protein interaction domains (GBD, SH3, and PDZ) to recruit three mevalonate biosynthetic enzymes (atoB, HMGS, and HMGR) C-terminally tagged with peptide ligands specific for these interaction domains. The number of interaction domain repeats in the scaffold can be varied as depicted by *x*, *y*, and *z*. (B) Enzymes with oligomeric structures could potentially bind multiple scaffolds, resulting in large complexes.

mevalonate production was observed with an optimal number (between 3 and 6) of SH3 ligands.

Use of a separate scaffold molecule enabled the addition of the first enzyme of this pathway, atoB, to the synthetic complex (Fig. 2A). When scaffolded, this pathway produced a 77-fold higher titer of mevalonate than it did when enzymes were not co-localized. Moreover, the scaffold with optimal architecture under low enzyme expression levels showed considerably faster growth and higher mevalonate titers than it did without scaffold under high induction of the pathway. The improvement was highly dependent on the scaffold architecture (i.e. number of interaction domain repeats and arrangement of these domains). However, the relationship between scaffold architecture and titer was not readily predictable. Our laboratory is currently investigating the specific mechanisms through which this pathway benefits from scaffolding (see Section 2.4).

The same strategy was applied to the three-enzyme glucaric acid pathway engineered by the Prather laboratory at MIT (Dueber et al., 2009; Moon et al., 2010). This pathway, which produces glucaric acid from glucose, presented an interesting challenge where the bottleneck enzyme, myo-inositol oxgenase (MIOX), appears to be activated by its substrate myo-inositol (Moon et al., 2009). Glucaric acid titer was improved five-fold by scaffolding, despite starting at a relatively high titer (~0.5 g/L). As was the case for the mevalonate pathway, scaffold architecture proved to be a critical parameter for optimizing pathway flux. Interestingly, there was a positive correlation between product titer and the number of interaction domains targeting the upstream enzyme, inositol-3-phosphate synthase (Ino1). This effect could be saturated at high numbers of targeting domains. In contrast, glucaric acid titer was not dependent on the number of interaction domains targeting the downstream enzyme, MIOX. Thus, in this case, the synthetic scaffold appears to improve glucaric acid titers by increasing the local concentration of myo-inositol around the substrate-activated enzyme, MIOX.

2.3. DNA-based scaffolds

DNA molecules have been investigated as another potential platform for organizing enzymes because DNA–DNA binding or DNA–protein specificity can be reliably accomplished with DNA hybridization or zinc-finger DNA binding domains, respectively. In one study, the enzymes glucose oxidase and horse radish peroxidase were covalently linked via a lysine residue to short DNA oligonucleotides that specifically hybridize onto polyhexagonal DNA nanostructures (Wilner et al., 2009). Although not the subject of their study, a slight but statistically significant increase in product formation was observed when the enzyme spacing was shortened from four hexagons (~33 nm apart) to two hexagons (~13 nm apart), suggesting that bringing pathway enzymes closer to one another does improve product formation. Unfortunately, the requirements to conjugate oligonucleotides onto enzymes and assemble DNA nanostructures make it impractical to implement this strategy *in vivo*. In a second example, the 2010 Slovenian international Genetically Engineered Machines (iGEM) team employed a plasmid scaffold to co-assemble the violacein biosynthetic enzymes (VioA-E) that were tethered to zinc finger DNA binding domains. When the pathway was scaffolded, they reported an approximately 6-fold increase in violacein production while the levels of deoxychromoviridans, the product of an undesirable side reaction, were significantly reduced (Dr. Roman Jerala, 2010 iGEM jamboree presentation). Plasmid scaffolds have the advantage of accommodating many interaction motifs and variable length linkers without solubility issues. A disadvantage of this strategy is that enzymes must be significantly modified with multiple zinc finger domains (usually 3–4 domains with a total addition of 90–120 amino acids, Collins et al., 2003). Additionally, the maximal concentration of DNA scaffolds in cell is limited by the maximal plasmid copy number (~500 per cell).

2.4. Mechanisms of synthetic scaffolds

While each of the pathways discussed above benefited significantly from enzyme scaffolding, the specific mechanisms contributing to product titer improvements have not been demonstrated conclusively. At this early stage, preliminary data is consistent with the possibility of a particularly interesting mechanism whereby scaffolding reduces the buildup of intermediates outside of scaffold complexes. This could occur if intermediates produced within the complex are quickly converted into product before a large portion of them escape the complex, similar to the naturally occurring "metabolite microdomains" (Baillie, 2009; Laude and Simpson, 2009; Selivanov et al., 2007). Thus far, indirect evidence appears consistent with this hypothesis. In the glucaric acid pathway, the positive correlation between titer and the number of Ino1 binding sites suggests that scaffolding increases the local intermediate concentration around the substrate activated enzyme, MIOX (Moon et al., 2010).

Scaffolding of the violacein pathway resulted in a decrease in side product formation, potentially due to reduced buildup of cross-reactive intermediates outside of the multi-enzyme complexes. In the mevalonate pathway, scaffolding enabled faster growth rates, likely by minimizing the cellular accumulation of the toxic intermediate HMG-CoA (Dueber et al., 2009). In the following section, we further explore the metabolite microdomain hypothesis, including a discussion of experiments to test it.

Metabolite microdomains are defined as regions with locally elevated concentrations of metabolites that are stable and persistent at steady state. Natural examples of such metabolite domains include Ca^{2+} microdomains (Laude and Simpson, 2009), cAMP microdomains (Baillie, 2009), and ATP microdomains (Selivanov et al., 2007). All of these phenomena are created by the co-localization of metabolite producers ("sources") and consumers ("sinks") such that the sinks consume free metabolites before the metabolites can diffuse an appreciable distance away from their sources (Fig. 3). For example, Ca^{2+} microdomains (Fig. 3A) are generated by localized Ca^{2+} ion channels (Ca^{2+} sources) surrounded by high concentrations of Ca^{2+} buffers (Ca^{2+} sinks). cAMP microdomains (Fig. 3B) form when adenyl cyclases (cAMP sources) and phosphodiesterases (cAMP sinks) are clustered by scaffolds. The presence of these microdomains has been directly visualized by fluorescent Ca^{2+} dyes or biosensors utilizing fluorescence resonance energy transfer (Zaccolo and Pozzan, 2002; Zenisek et al., 2003). Strikingly, the high [cAMP] can only be detected when the cAMP biosensors are targeted within the microdomains, but not when the biosensors are evenly distributed in the cytosol, demonstrating the steep cAMP gradient (Zaccolo and Pozzan, 2002). Other microdomains have also been observed. For example, ATP microdomains in heart muscles are established between creatine kinases (ATP sources) and myosin ATPase (ATP sinks) located adjacent to each other in myocytes (Selivanov et al., 2007). Scaffolded metabolic pathways are analogous to these natural systems in that enzymes catalyzing successive reactions are clustered and function as sources and sinks for intermediate metabolites (Fig. 3C).

Since the key for metabolite microdomain formation is to quickly consume intermediates before they escape from the complex, the higher the intermediate consumption rate (k) and/or the lower the intermediate diffusion coefficient (D), the easier it is to confine intermediates to small volumes. Models (W. Chen et al., 2008a, b; Neher, 1998) and experimental studies (Naraghi, 1997) of natural metabolite microdomains have shown that microdomain size is on the order of the square root of the metabolite diffusion coefficient over its consumption rate constant ($\sqrt{D/k}$). For both Ca^{2+} and cAMP microdomains, where the metabolite diffusion coefficients are approximately 100 $\mu m^2/s$ and the consumption rates are around 10^4–$10^5\ s^{-1}$, this model predicts a microdomain size of 100 nm, consistent with experimental findings (Meinrenken et al., 2002). In order for microdomains to be formed by scaffolding, the size of the scaffold complex must be greater than or equal to the predicted microdomain size. For the intermediate HMG-CoA and the moderately fast downstream enzyme HMGR,

$$D \approx 100\,\mu m^2/s, \frac{k_{cat}}{K_M} \approx 10^6\,M^{-1}\,s^{-1}$$

$$k = \frac{V_{max}}{K_M} = \frac{k_{cat}}{K_M}[E] \text{ (where } [E] \text{ is the enzyme concentration)}$$

Based on these constants, we can estimate $\sqrt{D/k} = \sqrt{100/[E]}$ nm. Enzymes clustered by synthetic scaffolds are spaced at a distance equal to the linker length plus the size of the protein-interaction domains, on the order of 5 nm, which is

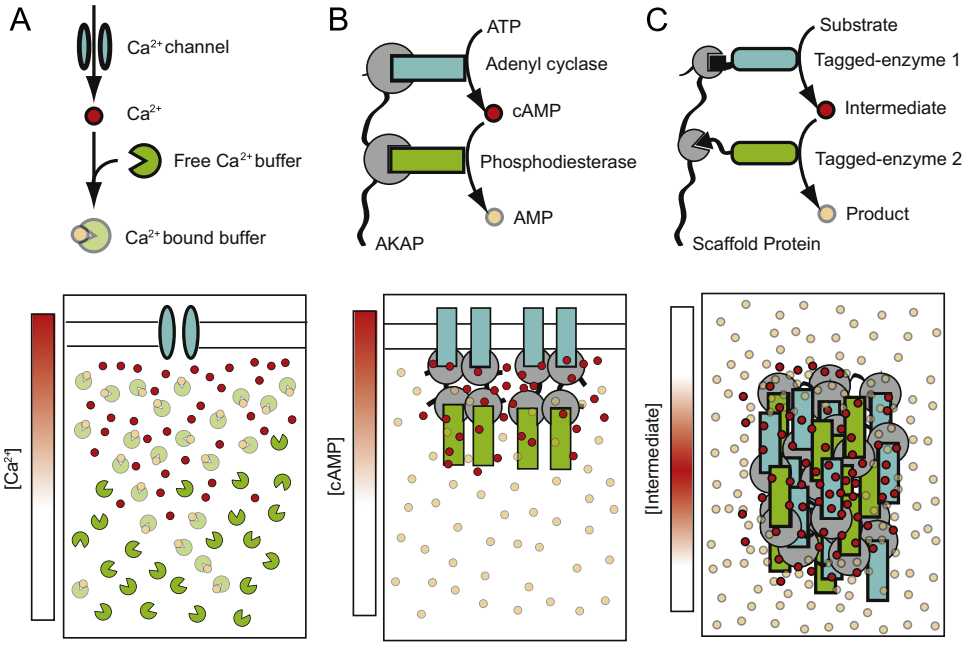

Fig. 3. Scaffolded enzyme complexes could form an intermediate microdomain analogous to Ca^{2+} and cAMP microdomains. Metabolite microdomains such as Ca^{2+} (A) or cAMP (B) microdomains are local regions of elevated metabolite concentration. They are characterized by co-localization of metabolite sources (e.g. Ca^{2+} channels and adenyl cyclases, blue) and sinks (e.g. Ca^{2+} buffers and phosphodiesterases, green) such that metabolites are produced (free Ca^{2+} and cAMP, red dots) and consumed (bound Ca^{2+} and AMP, dim yellow dots) locally. These domains are estimated to be less than 100 nm wide. In the case of cAMP microdomains, adenyl cyclases and phosphodiesterases are held together by A-kinase anchoring proteins (AKAPs, gray), a natural enzyme scaffold. In order to ensure few metabolites escape the microdomain, metabolite sinks are present at high concentrations around the sources. Mathematical modeling of cAMP microdomains suggests that multiple source and sink enzymes are required. Moreover, evidence exists that certain adenyl cyclases, phosphodiesterases, and AKAPs form oligomers. Synthetically scaffolded enzyme assemblies mimic this organization and may enable the formation of a microdomain of a pathway intermediate in a controlled manner (C). Since each subunit of an enzyme oligomer has a fused tag that binds synthetic scaffolds, multiple synthetic scaffolds can potentially be linked together to create large complexes that may provide the required enzyme concentration to significantly impede intermediate loss from the complex (see text for more detail). (For interpretation of the references to colour in this figure legend, the reader is referred to the web version of this article.)

equivalent to an enzyme concentration of 10^{-2} M. For these parameter estimates, we would predict that a complex $\geq$100 nm in size would generate an HMG-CoA microdomain. Although many of these parameters could differ significantly *in vivo*, unless the estimated D/k ratio is off by more than two orders of magnitude, the scaffolded protein complexes need to be bigger than a single scaffold – enzyme assembly to form metabolite microdomains.

Since many metabolic enzymes, including those in the mevalonate and glucaric acid pathways, are oligomeric, each enzyme oligomer likely brings together several scaffolds. At the same time, each scaffold binds multiple enzymes. Correspondingly, we predict that for functional scaffold architectures these binding events could induce the formation of large complexes, consisting of many enzymes and scaffolds (Fig. 2B). This kind of multimerization of proteins is not unprecedented. The formation of large protein complexes through scaffolding has been observed in nature. In the example of cAMP microdomains mentioned above, evidence exists that adenyl cyclases, phosphodiesterases, and the scaffold A-kinase anchoring proteins (AKAPs) form oligomers (Cooper and Crossthwaite, 2006; Gao et al., 2011; Richter and Conti, 2002), suggesting the possibility of multimeric protein complex formation. Another well-studied example is the postsynaptic density (PSD) in neurons, where scaffolds multimerize to create a high-order complex that clusters an extremely high density of adhesion proteins, neurotransmitter receptors, and signaling proteins (reviewed in Sheng and Hoogenraad, 2007). These protein clusters are particularly prominent in electron micrographs, appearing as a band of electron dense material around 300 nm in diameter and 25–50 nm in thickness. The estimated molecular weight of a PSD is about 1 GDa, thus containing on the order of 10^4 proteins (Chen et al., 2005). While we don't know the size of our synthetic scaffold complexes, reaching a comparable size to PSD's (hundreds of nanometers) is an intriguing possibility as this would be on the order of the size of Ca^{2+} and cAMP microdomains.

It should be noted that this model for intermediate microdomains breaks down if an intermediate's downstream enzyme is not in a diffusion-limited regime (and is instead fully saturated by intermediates). In this case, we predict that intermediates would leak out of the complex at high rates and prevent the formation of microdomains. Thus, this potential scaffolding mechanism is most likely only applicable to pathways with efficient downstream enzymes.

Whether this hypothesis represents a true mechanism by which scaffolds improve product titers in previously reported systems remains to be shown. Intermediate microdomains can be investigated with various kinetic approaches traditionally used to investigate substrate channeling. Electron microscopy and super-resolution light-microscopy (Toomre and Bewersdorf, 2010) may enable direct visualization of hundred-nanometer scale enzyme – scaffold complexes. Development of fluorescent dyes or biosensors specific to an intermediate of interest could allow *in vivo* imaging of microdomains, in the same way that Ca^{2+} microdomains are observed by fluorescent Ca^{2+} dyes (Zenisek et al., 2003) and cAMP microdomains by cAMP biosensors (Zaccolo and Pozzan, 2002).

In summary, synthetic scaffolds offer a modular tool for rationally clustering enzymes with stoichiometric control. Scaffolding has improved product titers in multiple cases, although the mechanism of action has yet to be elucidated experimentally. One mechanism of particular interest is the formation of intermediate microdomains, where enzyme – scaffold complexes reduce intermediate buildup by limiting the amount of intermediate that can escape the complex. Such a mechanism is appealing because it suggests that scaffolding could significantly benefit pathways with toxic intermediates (e.g. HMG-CoA), substrate activated enzymes (e.g. MIOX), or intermediates prone to be lost to undesirable side reactions or secreted from the cell. Our model for intermediate microdomains predicts that they could only exist if scaffolding generated large enzyme – scaffold complexes that were extremely enzyme dense. The formation of such complexes seems plausible based on our limited understanding, but other mechanisms should certainly be considered and tested. Among other potential mechanisms, scaffolds may prevent enzyme aggregation, increase enzymatic activity, or sterically block uncharacterized protein interactions (e.g. regulatory protein binding or protein degradation). Our laboratory and others are currently working to differentiate between these mechanisms.

3. Physical compartments for pathway sequestration

Regardless of the mechanisms at work in scaffolded systems, a more direct approach for limiting cross-talk between engineered pathways and the cellular milieu is to physically encapsulate pathway enzymes into distinct compartments. As discussed previously, compartmentalization is observed at the molecular level in substrate-channeling enzymes all the way up to organelles in eukaryotic cells. Compartmentalized pathways benefit from physical barriers that prevent metabolite exchange and protect heterologous enzymes from undesirable interactions with the host cell. Naturally occurring protein shells are a particularly attractive system for generating such compartments, as they have been shown to self-assemble in heterologous organisms and can be loaded with heterologous cargo. Additionally, pores on shell proteins could act as check points to selectively regulate metabolite entry and exit. An impressive list of protein shell structures has been discovered in nature: bacterial microcompartments (Yeates et al., 2008, 2010), smaller protein shells such as the lumazine synthase complex (Bacher et al., 1980) encapsulins (Sutter et al., 2008), and finally the eukaryotic ribonucleoprotein particle vault (Kedersha and Rome, 1986) (Fig. 4). Below, we briefly describe these shell proteins and discuss their potential as a tool for compartmentalizing engineered pathways.

3.1. Prokaryotic protein-based compartments

It is becoming increasingly appreciated that even though bacteria lack membrane-bound organelles, their interiors can contain various protein-based compartments. Many of these protein compartments are not well characterized; however, three classes of prokaryotic protein shells have received significant attention in the literature. The larger of the three is bacterial microcompartments (BMCs), a family of 80–200 nm proteinaceous polyhedra that typically encapsulate two or more sequential pathway enzymes at high copy numbers (10^2–10^3 per shell). While the enzymes encapsulated by BMCs differ greatly among bacterial species, all BMCs are composed of multiple evolutionarily related proteins that co-assemble to form their thin protein shells. Multiple examples of smaller protein shells, such as lumazine synthase and encapsulins, have also been fairly well characterized in prokaryotes. While forming similar polyhedral structures to BMCs, encapsulins and lumazine synthase complexes are only one-third the size (in diameter), spanning less than 30 nm, and are composed of 60–180 subunits of a single protein. In their natural contexts, these smaller compartments contain only a single type of enzyme at low copy numbers ($\sim$10 per shell).

Enzymes residing in both BMCs and smaller protein shells are thought to be incorporated into the complex during assembly of shell proteins, meaning that no additional enzymes can be imported after the compartments are formed. Metabolites can still traverse these compartments through $\sim$0.5 nm pores found

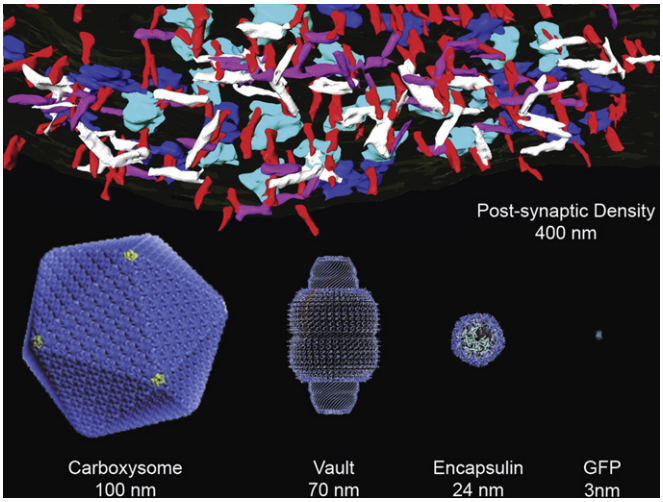

Fig. 4. Comparison of naturally occurring multi-enzyme complexes. (Top) The post-synaptic density (PSD) is a dense protein network just beneath the plasma membrane of neurons that forms a disk-like structure about 300–400 nm in diameter and 25–50 nm thick. This picture is a thin-sectioned EM reconstruction (adapted from X. Chen et al., 2008a, 2008b. Copyright (2008) National Academy of Sciences, USA) of a PSD. The backbone of PSD is a grid of cross-linked scaffold proteins, which are pseudo-colored here based on their orientations and shapes. Residing in these scaffolds are high densities of adhesion molecules, neurotransmitter receptors, and signaling proteins. (Bottom) Protein shells compartmentalize enzymes and limit metabolite diffusion across the shell. Carboxysomes (left, adapted from Tanaka et al., 2008. Copyright (2008) American Association for the Advancement of Science. Used with permission.) are part of the bacterial microcompartment (BMC) family of polyhedral protein complexes around 100 nm in diameter. Vaults (middle, adapted from Tanaka et al., 2009. Copyright (2009) American Association for the Advancement of Science. Used with permission.) are a ribonucleoprotein particle found in eukaryotes that measure 70 nm in height and 40 nm in width. Encapsulin (right, adapted from Sutter et al., 2008. Copyright (2008) Nature Publishing Group. Used with permission.) and the similarly sized lumazine synthase are also icosahedral protein complexes, but at 25 nm in diameter, they are much smaller than BMCs. Although BMCs can accommodate hundreds to thousands of proteins, balanced expression of multiple proteins is required for heterologous shell formation. In contrast, encapuslins are formed by a single shell protein, but can only accommodate ~10 proteins. Pores about 0.5 nm wide exist on most prokaryotic protein shells and are thought to selectively regulate metabolite entry and exit. By comparison, vaults have a 2.9 nm opening on each cap, which is unlikely to be very selective and are known to dynamically open and close by binding and unbinding at the waist. Vaults can carry tens of proteins and only require a single gene for assembly. GFP is included here as a point of reference.

on the shells. Some of these pores have been shown to be selective and are hypothesized to function as gates that regulate metabolite entry and exit. Pore selectivity makes protein-based prokaryotic compartments suitable candidates for spatially segregating metabolic pathways since enzymes can be sequestered into a region where metabolite access can be regulated. Specific strategies for engineering such systems are discussed below.

3.1.1. Protein sequestration into BMCs

At ~100 nm in diameter, BMCs are the largest known protein shells, capable of housing hundreds to thousands of enzymes (Yeates et al., 2008, 2010). For example, carboxysomes are estimated to contain 270 ribulose-1,5-bisphosphate carboxylase oxygenase (RuBisCO), a total of 4,320 subunits (Iancu et al., 2007; Shively and English, 1991). While the carboxysome is the most studied of all the BMCs, its expression in industrial hosts has yet to be achieved. Empty carboxysome shells without RuBisCO have been constructed, but the only protein sequestered thus far is heterologous RuBisCO (Menon et al., 2008). In contrast, Pdu shells can be generated in *E. coli* by expressing just six shell proteins (Parsons et al., 2010), and an 18 amino-acid N-terminal peptide is sufficient for sequestering green fluorescent proteins (GFP) or glutathione S-transferase (GST) into Pdu (Fan et al., 2010). Immunoprecipitation or pull-down assays showed that the encapsulated GFP or GST are not accessible to corresponding antibodies or glutathione beads, respectively. These advances may make Pdu a more immediate target for metabolic engineering. Additional studies of natural Pdu enzymes may yield a larger set of targeting sequences for encapsulating multiple enzymes. Sequestration of heterologous enzymes could be quickly assayed *in vivo* by monitoring the degree of protection from protein degradation after adding an N- or C-terminal degron to an enzyme of interest (Flynn et al., 2003; Sauer et al., 2004).

3.1.2. Protein sequestration into lumazine synthase and encapsulins

Lumazine synthase complexes (Bacher et al., 1980) and encapsulins (Sutter et al., 2008) are smaller polyhedral protein complexes with an interior diameter of 10–25 nm and a 2.5 nm thick shell. Each complex consists of either 60 or 180 shell protein subunits encoded by a single gene. In the case of lumazine synthase, both the 60-subunit and 180-subunit compositions are possible depending on the cellular environment. Regardless of the subunit composition, these smaller shells can only hold few copies of enzymes: a single lumazine synthase complex (60-subunit version) contains three riboflavin synthases (Bacher et al., 1980); *Brevibacterium linens* encapsulin houses a single peroxidase hexamer (DyP); *Thermotoga maritima* encapsulin can store twelve of the smaller Flp (ferritin-like proteins) decamers (Sutter et al., 2008). As was the case for BMCs, natural cargo is not necessary for shell assembly (Schott et al., 1990; Sutter et al., 2008). Cargo targeting has been studied for both encapsulins and lumazine synthase. A conserved sequence near the C-terminus of endogenous enzymes is required for protein sequestration into encapsulins (Sutter et al., 2008). While it remains to be determined whether this sequence is sufficient for targeting heterologous proteins, it is hypothesized that the protein targeting signal can be deduced from the sequence of endogenous enzymes and insights gained from the crystal structure (Sutter et al., 2008). The natural targeting signal for lumazine synthase has yet to be found. However, four negatively charged residues inserted into the loops of each lumazine synthase subunit are sufficient to recruit GFP (Seebeck et al., 2006) and HIV protease (Wörsdörfer et al., 2011) tagged with ten positively charged amino acids. As expected, the loading capacity was low: ~3.5 GFP's and ~1 protease per lumazine synthase (180-subunit version). Worsdorfer et al. utilized the toxicity of HIV protease to increase the loading capacity of lumazine synthase 5–10 fold through directed evolution (Wörsdörfer et al., 2011). Improvements were found to be the result of increases in negatively charged residues or neutralization of positively charged residues in the interior of lumazine synthase, most likely due to an increased binding affinity to the positively charged tag on HIV protease. Even after optimization, the low enzyme capacity of these smaller protein shells should be taken into consideration, especially for applications requiring the sequestration of multiple pathway enzymes. Regardless, these advances demonstrate that these shells are somewhat plastic and can be tailored for cargo of interest.

3.1.3. Metabolite transport into prokaryotic protein-based compartments

Prokaryotic protein-based compartments are known to regulate metabolite access to the interior of the microcompartments. Carboxysomes are thought to impede CO_2 and O_2 diffusion such that CO_2 is concentrated around the relatively inefficient RuBisCO, while the import of O_2, a competitive substrate for RuBisCO, is limited (Dou et al., 2008; Marcus et al., 1992). Pdu traps toxic aldehyde

intermediates inside its shell (Sampson and Bobik, 2008). Lumazine synthase channels its intermediate, 6,7-dimethyl-8-ribityllumazine, between the shell and the sequestered native enzymes. While intermediates and inhibitors are prevented from diffusing across the shell, native substrates and products appear to easily enter and exit the compartments. Structural data indicates that canonical BMC shell proteins form hexamers with a 0.4–0.6 nm pore located at the center, which may provide selective entry to the microcompartments (Crowley et al., 2008; Kerfeld et al., 2005; Tsai et al., 2007). Similar sized pores are also found on encapsulins (Sutter et al., 2008). The sizes of the pores are big enough to allow most small molecules to pass, so it is unclear how intermediates are blocked. It has been proposed that positive charges around the pores of carboxysomes attract negatively charged substrate, (bicarbonate, HCO_3^-) but not CO_2 or O_2 (Kerfeld et al., 2005). Open and closed pore structures have been solved for some shell proteins (Klein et al., 2009; Sagermann et al., 2009; Tanaka et al., 2010), suggesting that the pores may dynamically control metabolite selectivity. Further biochemical studies of pore function will aid in engineering shells with new metabolite selectivity.

3.1.4. Screening for desired transport selectivity in prokaryotic protein-based compartments

Since shell selectivity is likely to be directly linked to amino acid composition at the pore, random mutations of the pore residues coupled with an effective screening or selection strategy should generate specificity based on metabolite size and/or charge. The development of methods to monitor the concentration of pathway metabolites is critical for such a screen to succeed. Transcriptional biosensors for desired metabolites, similar to the mevalonate responsive regulator protein engineered from AraC (Tang and Cirino, 2010), could be used to select for or against the presence of that metabolite. Bacteria have a large number of effector-binding transcriptional regulators that are specific for a wide range of metabolites. Mutagenesis and DNA shuffling have been used to engineer new effector specificities (Galvão and de Lorenzo, 2006). By coupling transcriptional regulators to the expression of an antibiotic resistance gene or a cytotoxic protein, positive or negative selections can be carried out for metabolites of interest. When the enzyme producing the metabolite of interest is sequestered into a protein shell, a negative selection for the metabolite would result in pores blocking the metabolite, while a positive selection would result in the opposite. Alternatively, FRET sensors could be engineered for pathway metabolites as was done for maltose and pentoses (Fehr et al., 2002; Kaper et al., 2008; Lager et al., 2003). When sequestered inside protein compartments, these sensors would allow direct measurement of metabolite permeability. It should be noted that since the shells of BMCs are encoded by multiple genes which all contribute to pore formation, it may be considerably harder to generate BMCs that block intermediates than it would be for lumazine synthase or encapsulins, whose shells are encoded by a single gene.

3.2. Eukaryotic protein-based compartment: vaults

A large ribonucleoprotein particle named "vault" has been isolated from rat liver as well as many other mammalian cell lines (Kedersha and Rome, 1986). Vaults are measured to be approximately $70 \times 40 \times 40\ nm^3$ and have the capacity to accommodate tens of proteins. Each vault consists of two symmetric halves (half vaults) connected at the middle (waist) (Fig. 4). Natural vaults contain three proteins and a small stretch of RNA, although only a single protein, major vault protein (MVP), is required for shell formation (Anderson et al., 2007). It is estimated that each vault carries ~2 copies of the 290 kDa telomerase associated protein 1 (TEP1) and ~11 copies of the 193 kDa vault poly(ADP-ribose) polymerase (VPARP) (Kong et al., 2000). A minimal interaction domain (mINT) for targeting cargo to vaults was identified in VPARP and used successfully to sequester GFP, mCherry, luciferase (Kickhoefer et al., 2005), Major Outer Membrane Protein (Champion et al., 2009), and adenovirus protein VI (Lai et al., 2009). Similar to the number of VPARPs in vaults, it was estimated that >9 copies of GFP-mINT can be sequestered into each vault (Goldsmith et al., 2009). Evidence suggests that vaults form a diffusion barrier against small molecules, especially those that are charged (Kickhoefer et al., 2005), potentially by restricting metabolite diffusion through the relatively large 2.9 nm opening located at the cap of each half vault (Anderson et al., 2007). Half vaults are known to rapidly dissociate and associate at the waist, which may temporarily expose the vault interior (Yang et al., 2010). Due to their large pore size and dynamic dissociation, vaults are predicted to provide higher levels of mixing with the cellular environment than would bacterial protein shells. This property may prove advantageous for systems limited by substrate availability within the complex.

In summary, the first steps of engineering on protein-based compartments for metabolic engineering applications have been achieved. Empty protein shells have been generated and targeted with heterologous cargo in the case of Pdu, lumazine synthase, and vaults. Shells differ in size and the ease with which they can be expressed in industrial hosts. The main challenge ahead will be to create pores that are selective so substrates and products can get through but intermediates cannot. While engineering small molecule selectivity is likely to be a challenging endeavor, selectivity seen in natural pores suggests this should be feasible. Positive and negative selections could be performed using engineered effector-binding transcription regulators. In addition, fluorescent sensors for metabolites may be used as a read-out for high throughput screening.

4. Conclusions

In this review, we've discussed two emerging strategies for spatially organizing metabolic pathways into multi-enzyme complexes: enzyme scaffolding and protein shells. Both have their potential advantages and associated challenges (Table 1). The modular nature of protein interaction domains allows relatively easy construction of synthetic scaffolds. Scaffolding has been used to improve product titer in multiple engineered pathways, and in each case, scaffold architecture proved to be a critical determinant of success. Although the specific mechanisms through which scaffolding increases product titers have not been demonstrated experimentally, one particularly interesting hypothesis is the formation of intermediate microdomains, which would arise if multi-enzyme complexes limited the accumulation of intermediates in the cellular milieu. Theoretical models of naturally occurring metabolite microdomains predict that scaffolding must form large complexes that are extremely enzyme-dense in order to generate such an effect. Natural scaffold proteins in the post-synaptic density create protein-rich complexes up to a few hundred nanometers wide. Similar complexes could exist in scaffolded systems due to the oligomeric nature of metabolic enzymes where each individual subunit has a scaffold-recruiting ligand such that multiple scaffolded complexes can co-assemble given suitable scaffold architectures. We predict that microdomains could only form for intermediates with a diffusion limited downstream enzyme, making this mechanism applicable only to a subset of metabolic pathways. Our laboratory and others are

Table 1
Comparison of the different strategies for organizing pathway enzymes into multi-protein complexes discussed in this review.

Type	Interior diameter (nm)	Minimal no. of subunits to form	No. of natural cargo proteins	No. of exogenous cargo proteins	Access to enzymes	Mechanism to limit intermediate buildup
Scaffold	300[a]	1[b]	10^3–10^4[c]	Not determined	Free diffusion	By quickly turning over intermediates
BMC	70–130	5[d] ,6[e]	$\sim 10^3$[f]	Not determined	Pores	Protein shell + selective pores
Vault	$60 \times 30 \times 30$	1	~ 11[g]	~ 9[h]	Cap pores and dynamic half-vault exchange	Protein shell + cap pores
Lumazine synthase and encapsulin	10–25	1	3[i], 6[j], 120[k]	3 [l], 7[m]	Pores	Protein shell + selective pores

[a] Based on the post-synaptic density (Sheng and Hoogenraad, 2007).
[b] Theoretically, only one synthetic scaffold binding to multiple oligomeric enzymes is required to form a large complex.
[c] Based on the post-synaptic density (Chen et al., 2005).
[d] Carboxysome (Menon et al., 2008).
[e] Pdu (Parsons et al., 2010).
[f] Carboxysome can hold 270 RuBisCO enzymes (4320 total subunits) (Iancu et al., 2007; Shively and English, 1991).
[g] Each vault is estimated to hold ~11 VPARP (Kong et al., 2000).
[h] Each vault can hold >9 GFP−mINT fusion proteins (Goldsmith et al., 2009).
[i] Lumazine synthase complexes hold 3 riboflavin synthases (Bacher et al., 1980).
[j] *B. linens* encapsulin holds one DyP hexamer (Sutter et al., 2008).
[k] *T. maritima* encapulin holds twelve Flp decamers (Sutter et al., 2008).
[l] Engineered lumazine synthase on averge can hold three GFPs (Seebeck et al., 2006).
[m] Engineered lumazine synthase can hold 7 HIV proteases after optimization (Wörsdörfer et al., 2011).

actively studying mechanisms such as this one in order to more fully characterize a set of design rules for enzyme scaffolding.

Protein shells provide the opportunity to encapsulate both pathway enzymes and intermediates with physical barriers. Many examples of protein-based compartments exist in nature that can be adapted for metabolic engineering, although it appears that tradeoffs must be made between shell complexity and cargo capacity. Bacterial microcompartments can accommodate many enzymes (10^2–10^3 per shell), but require the balanced expression of 5–6 different proteins for proper assembly. Smaller protein shells like encapsulin are formed by a single gene but have limited cargo capacity (1–10 enzymes per shell). Vaults combine the simple shell composition of encapsulin with a slightly larger cargo capacity (~10 200 kDa proteins per shell), but are likely to suffer from poor metabolite selectivity. Specific targeting sequences have been discovered for many of these compartments, but additional targeting sequences and/or scaffold targeting will be necessary to gain stoichiometric control over compartmentalized pathways. In order to maximize the benefit of compartmentalization, engineering pores to selectively control metabolite diffusion is critical but will likely be challenging. Eventually, we envision modular compartments that can accommodate entire synthetic pathways and serve to minimize unwanted cross-talk between the synthetic pathways and the industrial host's metabolism. Confining pathways to compartments should mitigate problems such as metabolite toxicity, uncharacterized allosteric regulation, and intermediate loss to side products or cell secretion. For pathways with diffusion-limited enzymes, flux should also increase due to higher local substrate concentrations. Together, these effects should significantly improve our ability to predictably engineer heterologous pathways to produce economically viable titers of renewable chemicals.

Update

While this article was under review, a new report (Delebecque et al., 2011) from Pamela Silver's laboratory demonstrated that RNA-based scaffold can be utilized *in vivo* to co-localize hydrogenases and ferrodoxins, which increases H_2 production by ~48-fold compared to non-scaffolded proteins. In this design, sequence-symmetric RNA building blocks were constructed to allow polymerization into one- or two-dimensional scaffolds isothermally. A PP7 and a MS2 aptamer domain were included in each RNA building block to bind PP7 and MS2 fusion proteins, respectively. Remarkably, the two-dimensional RNA scaffolds formed stable ~100 nm sphere-like structures in cells, and allowed fusion proteins to cluster in close proximity as demonstrated by fluorescence complementation experiments. It is important to point out that in this hydrogen production pathway, electrons are transferred from reduced ferrodoxins to protons resulting in hydrogen formation. Hence, ferrodoxin is a substrate of hydrogenase and no intermediate metabolites are produced. Thus, the increase of hydrogen yield may be explained by an increase of collision frequency between ferrodoxins and hydrogenases when they are clustered by the RNA scaffolds.

Acknowledgments

The authors would like to thank Stanley Lei Qi, Weston Whitaker, Michael Lee, Katelyn Connell and the rest of the Dueber laboratory for discussions in preparing this review. This work is supported by Energy Biosciences Institute to Hanson Lee, by Graduate Research Fellowship from National Science Foundation to William DeLoache, and by National Science Foundation to John Dueber (Grant # CBET-0756801).

References

An, S., Kumar, R., Sheets, E.D., Benkovic, S.J., 2008. Reversible compartmentalization of de novo purine biosynthetic complexes in living cells. Science 320, 103–106.
Anderson, D.H., Kickhoefer, V.A., Sievers, S.A., Rome, L.H., Eisenberg, D., 2007. Draft crystal structure of the vault shell at 9-Å resolution. PLoS Biol. 5, e318.
Bacher, A., Baur, R., Eggers, U., Harders, H.D., Otto, M.K., Schnepple, H., 1980. Riboflavin synthases of *Bacillus subtilis*. Purification and properties. J. Biol. Chem. 255, 632–637.
Baillie, G.S., 2009. Compartmentalized signalling: spatial regulation of cAMP by the action of compartmentalized phosphodiesterases. FEBS J. 276, 1790–1799.

Champion, C.I., Kickhoefer, V.A., Liu, G., Moniz, R.J., Freed, A.S., Bergmann, L.L., Vaccari, D., Raval-Fernandes, S., Chan, A.M., Rome, L.H., Kelly, K.A., 2009. A vault nanoparticle vaccine induces protective mucosal immunity. PLoS ONE 4, e5409.

Chen, W., Levine, H., Rappel, W.-J., 2008a. A mathematical analysis of second messenger compartmentalization. Phys. Biol. 5, 046006.

Chen, X., Vinade, L., Leapman, R.D., Petersen, J.D., Nakagawa, T., Phillips, T.M., Sheng, M., Reese, T.S., 2005. Mass of the postsynaptic density and enumeration of three key molecules. Proc. Nat. Acad. Sci. US A 102, 11551–11556.

Chen, X., Winters, C., Azzam, R., Li, X., Galbraith, J.A., Leapman, R.D., Reese, T.S., 2008b. Organization of the core structure of the postsynaptic density. Proc. Nat. Acad. Sci. 105, 4453–4458.

Collins, C.H., Yokobayashi, Y., Umeno, D., Arnold, F.H., 2003. Engineering proteins that bind, move, make and break DNA. Curr. Opin. Biotechnol. 14, 371–378.

Conrado, R.J., Varner, J.D., DeLisa, M.P., 2008. Engineering the spatial organization of metabolic enzymes: mimicking nature's synergy. Curr. Opin. Biotechnol. 19, 492–499.

Cooper, D.M.F., Crossthwaite, A.J., 2006. Higher-order organization and regulation of adenylyl cyclases. Trends Pharmacol. Sci. 27, 426–431.

Crowley, C.S., Sawaya, M.R., Bobik, T.A., Yeates, T.O., 2008. Structure of the PduU shell protein from the Pdu microcompartment of *Salmonella*. Structure 16, 1324–1332.

Delebecque, C.J., Lindner, A.B., Silver, P.A., Aldaye, F.A., 2011. Organization of intracellular reactions with rationally designed RNA assemblies. Science.

Dou, Z., Heinhorst, S., Williams, E.B., Murin, C.D., Shively, J.M., Cannon, G.C., 2008. CO_2 fixation kinetics of *Halothiobacillus neapolitanus* mutant carboxysomes lacking carbonic anhydrase suggest the shell acts as a diffusional barrier for CO_2. J. Biol. Chem. 283, 10377–10384.

Dueber, J.E., Wu, G.C., Malmirchegini, G.R., Moon, T.S., Petzold, C.J., Ullal, A.V., Prather, K.L.J., Keasling, J.D., 2009. Synthetic protein scaffolds provide modular control over metabolic flux. Nat. Biotech. 27, 753–759.

Dueber, J.E., Yeh, B.J., Bhattacharyya, R.P., Lim, W.A., 2004. Rewiring cell signaling: the logic and plasticity of eukaryotic protein circuitry. Curr. Opin. Struct. Biol. 14, 690–699.

Fan, C., Cheng, S., Liu, Y., Escobar, C.M., Crowley, C.S., Jefferson, R.E., Yeates, T.O., Bobik, T.A., 2010. Short N-terminal sequences package proteins into bacterial microcompartments. Proc. Nat. Acad. Sci. 107, 7509–7514.

Fehr, M., Frommer, W.B., Lalonde, S., 2002. Visualization of maltose uptake in living yeast cells by fluorescent nanosensors. Proc. Nat. Acad. Sci. USA 99, 9846–9851.

Flynn, J.M., Neher, S.B., Kim, Y.-I., Sauer, R.T., Baker, T.A., 2003. Proteomic discovery of cellular substrates of the ClpXP protease reveals five classes of ClpX-recognition signals. Mol. Cell 11, 671–683.

Galvão, T.C., de Lorenzo, V., 2006. Transcriptional regulators à la carte: engineering new effector specificities in bacterial regulatory proteins. Curr. Opin. Biotechnol. 17, 34–42.

Gao, S., Wang, H.-Y., Malbon, C.C., 2011. AKAP5 and AKAP12 form homo-oligomers. J. Mol. Signal. 6 3-3.

Goldsmith, L.E., Pupols, M., Kickhoefer, V.A., Rome, L.H., Monbouquette, H.G., 2009. Utilization of a protein "Shuttle" to load vault nanocapsules with gold probes and proteins. ACS Nano 3, 3175–3183.

Iancu, C.V., Ding, H.J., Morris, D.M., Dias, D.P., Gonzales, A.D., Martino, A., Jensen, G.J., 2007. The structure of isolated *Synechococcus* strain WH8102 carboxysomes as revealed by electron cryotomography. J. Mol. Biol. 372, 764–773.

Kaper, T., Lager, I., Looger, L., Chermak, D., Frommer, W., 2008. Fluorescence resonance energy transfer sensors for quantitative monitoring of pentose and disaccharide accumulation in bacteria. Biotechnol. Biofuels 1, 11.

Keasling, J.D., 2010. Manufacturing molecules through metabolic engineering. Science 330, 1355–1358.

Kedersha, N.L., Rome, L.H., 1986. Isolation and characterization of a novel ribonucleoprotein particle: large structures contain a single species of small RNA. J. Cell Biol. 103, 699–709.

Kerfeld, C.A., Sawaya, M.R., Tanaka, S., Nguyen, C.V., Phillips, M., Beeby, M., Yeates, T.O., 2005. Protein structures forming the shell of primitive bacterial organelles. Science 309, 936–938.

Kickhoefer, V.A., Garcia, Y., Mikyas, Y., Johansson, E., Zhou, J.C., Raval-Fernandes, S., Minoofar, P., Zink, J.I., Dunn, B., Stewart, P.L., Rome, L.H., 2005. Engineering of vault nanocapsules with enzymatic and fluorescent properties. Proc. Nat. Acad. Sci. USA 102, 4348–4352.

Kizer, L., Pitera, D.J., Pfleger, B.F., Keasling, J.D., 2008. Application of functional genomics to pathway optimization for increased isoprenoid production. Appl. Environ. Microbiol. 74, 3229–3241.

Klein, M.G., Zwart, P., Bagby, S.C., Cai, F., Chisholm, S.W., Heinhorst, S., Cannon, G.C., Kerfeld, C.A., 2009. Identification and structural analysis of a novel carboxysome shell protein with implications for metabolite transport. J. Mol. Biol. 392, 319–333.

Kong, L.B., Siva, A.C., Kickhoefer, V.A., Rome, L.H., Stewart, P.L., 2000. RNA location and modeling of a WD40 repeat domain within the vault. RNA 6, 890–900.

Lager, I., Fehr, M., Frommer, W.B., Lalonde, S., 2003. Development of a fluorescent nanosensor for ribose. FEBS Lett. 553, 85–89.

Lai, C.-Y., Wiethoff, C.M., Kickhoefer, V.A., Rome, L.H., Nemerow, G.R., 2009. Vault nanoparticles containing an adenovirus-derived membrane lytic protein facilitate toxin and gene transfer. ACS Nano 3, 691–699.

Laude, A.J., Simpson, A.W.M., 2009. Compartmentalized signalling: Ca^{2+} compartments, microdomains and the many facets of Ca^{2+} signalling. FEBS J. 276, 1800–1816.

Maeder, M.L., Thibodeau-Beganny, S., Osiak, A., Wright, D.A., Anthony, R.M., Eichtinger, M., Jiang, T., Foley, J.E., Winfrey, R.J., Townsend, J.A., Unger-Wallace, E., Sander, J.D., Muller-Lerch, F., Fu, F., Pearlberg, J., Gobel, C., Dassie, J.P., Pruett-Miller, S.M., Porteus, M.H., Sgroi, D.C., Iafrate, A.J., Dobbs, D., McCray Jr., P.B., Cathomen, T., Voytas, D.F., Joung, J.K., 2008. Rapid "open-source" engineering of customized zinc-finger nucleases for highly efficient gene modification. Mol. Cell 31, 294–301.

Marcus, Y., Berry, J., Pierce, J., 1992. Photosynthesis and photorespiration in a mutant of the cyanobacterium Synechocystis PCC 6803 lacking carboxysomes. Planta, 187.

Meinrenken, C.J., Borst, J.G.G., Sakmann, B., 2002. Calcium secretion coupling at calyx of held governed by nonuniform channel-vesicle topography. J. Neurosci. 22, 1648–1667.

Menon, B.B., Dou, Z., Heinhorst, S., Shively, J.M., Cannon, G.C., 2008. *Halothiobacillus neapolitanus* carboxysomes sequester heterologous and chimeric rubisco species. PLoS ONE 3, e3570.

Miles, E.W., 2001. Tryptophan synthase: a multienzyme complex with an intramolecular tunnel. Chem. Rec. (New York, NY) 1, 140–151.

Moon, T.S., Dueber, J.E., Shiue, E., Prather, K.L.J., 2010. Use of modular, synthetic scaffolds for improved production of glucaric acid in engineered *E. coli*. Metab. Eng. 12, 298–305.

Moon, T.S., Yoon, S.-H., Lanza, A.M., Roy-Mayhew, J.D., Prather, K.L.J., 2009. Production of glucaric acid from a synthetic pathway in recombinant *Escherichia coli*. Appl. Environ. Microbiol. 75, 589–595.

Naraghi, M., 1997. T-jump study of calcium binding kinetics of calcium chelators. Cell Calcium 22, 255–268.

Narayanaswamy, R., Levy, M., Tsechansky, M., Stovall, G.M., O'Connell, J.D., Mirrielees, J., Ellington, A.D., Marcotte, E.M., 2009. Widespread reorganization of metabolic enzymes into reversible assemblies upon nutrient starvation. Proc. Nat. Acad. Sci. 106, 10147–10152.

Neher, E., 1998. Usefulness and limitations of linear approximations to the understanding of Ca^{++} signals. Cell Calcium 24, 345–357.

Noree, C., Sato, B.K., Broyer, R.M., Wilhelm, J.E., 2010. Identification of novel filament-forming proteins in *Saccharomyces cerevisiae* and *Drosophila melanogaster*. J. Cell Biol. 190, 541–551.

Parsons, J.B., Frank, S., Bhella, D., Liang, M., Prentice, M.B., Mulvihill, D.P., Warren, M.J., 2010. Synthesis of empty bacterial microcompartments, directed organelle protein incorporation, and evidence of filament-associated organelle movement. Mol. Cell 38, 305–315.

Pawson, T., Nash, P., 2000. Protein-protein interactions define specificity in signal transduction. Genes Dev. 14, 1027–1047.

Peisajovich, S.G., Garbarino, J.E., Wei, P., Lim, W.A., 2010. Rapid diversification of cell signaling phenotypes by modular domain recombination. Science 328, 368–372.

Pitera, D.J., Paddon, C.J., Newman, J.D., Keasling, J.D., 2007. Balancing a heterologous mevalonate pathway for improved isoprenoid production in *Escherichia coli*. Metab. Eng.. 9, 193–207.

Posern, G., Zheng, J., Knudsen, B.S., Kardinal, C., Müller, K.B., Voss, J., Shishido, T., Cowburn, D., Cheng, G., Wang, B., Kruh, G.D., Burrell, S.K., Jacobson, C.A., Lenz, D.M., Zamborelli, T.J., Adermann, K., Hanafusa, H., Feller, S.M., 1998. Development of highly selective SH3 binding peptides for Crk and CRKL which disrupt Crk-complexes with DOCK180, SoS and C3G. Oncogene 16, 1903–1912.

Remenyi, A., Good, M.C., Lim, W.A., 2006. Docking interactions in protein kinase and phosphatase networks. Curr. Opin. Struct. Biol. 16, 676–685.

Richter, W., Conti, M., 2002. Dimerization of the type 4 cAMP-specific phosphodiesterases is mediated by the upstream conserved regions (UCRs). J. Biol. Chem. 277, 40212–40221.

Sagermann, M., Ohtaki, A., Nikolakakis, K., 2009. Crystal structure of the EutL shell protein of the ethanolamine ammonia lyase microcompartment. Proc. Nat. Acad. Sci. 106, 8883–8887.

Sampson, E.M., Bobik, T.A., 2008. Microcompartments for B12-dependent 1,2-propanediol degradation provide protection from DNA and cellular damage by a reactive metabolic intermediate. J. Bacteriol. 190, 2966–2971.

Sauer, R.T., Bolon, D.N., Burton, B.M., Burton, R.E., Flynn, J.M., Grant, R.A., Hersch, G.L., Joshi, S.A., Kenniston, J.A., Levchenko, I., Neher, S.B., Oakes, E.S.C., Siddiqui, S.M., Wah, D.A., Baker, T.A., 2004. Sculpting the proteome with AAA+ proteases and disassembly machines. Cell 119, 9–18.

Schott, K., Ladenstein, R., König, A., Bacher, A., 1990. The lumazine synthase-riboflavin synthase complex of Bacillus subtilis. Crystallization of reconstituted icosahedral beta-subunit capsids. J. Biol. Chem. 265, 12686–12689.

Seebeck, F.P., Woycechowsky, K.J., Zhuang, W., Rabe, J.P., Hilvert, D., 2006. A simple tagging system for protein encapsulation. J. Am. Chem. Soc. 128, 4516–4517.

Selivanov, V.A., Krause, S., Roca, J., Cascante, M., 2007. Modeling of spatial metabolite distributions in the cardiac sarcomere. Biophys. J. 92, 3492–3500.

Sheng, M., Hoogenraad, C.C., 2007. The postsynaptic architecture of excitatory synapses: a more quantitative view. Annu. Rev. Biochem. 76, 823–847.

Shively, J.M., English, R.S., 1991. The carboxysome, a prokaryotic organelle: a mini-review. Can. J. Botany 69, 957–962.

Sutter, M., Boehringer, D., Gutmann, S., Gunther, S., Prangishvili, D., Loessner, M.J., Stetter, K.O., Weber-Ban, E., Ban, N., 2008. Structural basis of enzyme encapsulation into a bacterial nanocompartment. Nat. Struct. Mol. Biol. 15, 939–947.

Tanaka, H., Kato, K., Yamashita, E., Sumizawa, T., Zhou, Y., Yao, M., Iwasaki, K., Yoshimura, M., Tsukihara, T., 2009. The structure of rat liver vault at 3.5 Angstrom resolution. Science 323, 384–388.

Tanaka, S., Kerfeld, C.A., Sawaya, M.R., Cai, F., Heinhorst, S., Cannon, G.C., Yeates, T.O., 2008. Atomic-level models of the bacterial carboxysome shell. Science 319, 1083–1086.

Tanaka, S., Sawaya, M.R., Yeates, T.O., 2010. Structure and mechanisms of a protein-based organelle in *Escherichia coli*. Science 327, 81–84.

Tang, S.-Y., Cirino, P.C., 2010. Design and application of a mevalonate-responsive regulatory protein. Angewandte Chemie (International Ed. in English).

Tonikian, R., Zhang, Y., Sazinsky, S.L., Currell, B., Yeh, J.-H., Reva, B., Held, H.A., Appleton, B.A., Evangelista, M., Wu, Y., Xin, X., Chan, A.C., Seshagiri, S., Lasky, L.A., Sander, C., Boone, C., Bader, G.D., Sidhu, S.S., 2008. A specificity map for the PDZ domain family. PLoS Biol. 6, e239.

Toomre, D., Bewersdorf, J., 2010. A new wave of cellular imaging. Annu. Rev. Cell Dev. Biol. 26, 285–314.

Tsai, Y., Sawaya, M.R., Cannon, G.C., Cai, F., Williams, E.B., Heinhorst, S., Kerfeld, C.A., Yeates, T.O., 2007. Structural analysis of CsoS1A and the protein shell of the *Halothiobacillus neapolitanus* carboxysome. PLoS Biol., 5.

Wilner, O.I., Weizmann, Y., Gill, R., Lioubashevski, O., Freeman, R., Willner, I., 2009. Enzyme cascades activated on topologically programmed DNA scaffolds. Nat Nano 4, 249–254.

Wörsdörfer, B., Woycechowsky, K.J., Hilvert, D., 2011. Directed evolution of a protein container. Science 331, 589–592.

Yang, J., Kickhoefer, V.A., Ng, B.C., Gopal, A., Bentolila, L.A., John, S., Tolbert, S.H., Rome, L.H., 2010. Vaults are dynamically unconstrained cytoplasmic nanoparticles capable of half vault exchange. ACS Nano 4, 7229–7240.

Yeates, T.O., Crowley, C.S., Tanaka, S., 2010. Bacterial microcompartment organelles: protein shell structure and evolution. Annu. Rev. Biophys. 39, 185–205.

Yeates, T.O., Kerfeld, C.A., Heinhorst, S., Cannon, G.C., Shively, J.M., 2008. Protein-based organelles in bacteria: carboxysomes and related microcompartments. Nat. Rev. Micro 6, 681–691.

Zaccolo, M., Pozzan, T., 2002. Discrete microdomains with high concentration of cAMP in stimulated rat neonatal cardiac myocytes. Science (New York, NY) 295, 1711–1715.

Zenisek, D., Davila, V., Wan, L., Almers, W., 2003. Imaging calcium entry sites and ribbon structures in two presynaptic cells. J. Neurosci. 23, 2538–2548.